



HAL
open science

Gonadotropin-releasing hormone stimulates the biosynthesis of pregnenolone sulfate and dehydroepiandrosterone sulfate in the hypothalamus

Delphine Burel, Jian Hua Li, Jean-Luc Do-Rego, Ai Fen Wang, Van Luu-The, Georges Pelletier, Yves Tillet, Catherine Taragnat, Hyuk Bang Kwon, Jae Young Seong, et al.

► To cite this version:

Delphine Burel, Jian Hua Li, Jean-Luc Do-Rego, Ai Fen Wang, Van Luu-The, et al.. Gonadotropin-releasing hormone stimulates the biosynthesis of pregnenolone sulfate and dehydroepiandrosterone sulfate in the hypothalamus. *Endocrinology*, 2013, 154 (6), pp.2114-2128. 10.1210/en.2013-1095 . hal-01129713

HAL Id: hal-01129713

<https://hal.science/hal-01129713>

Submitted on 28 May 2020

HAL is a multi-disciplinary open access archive for the deposit and dissemination of scientific research documents, whether they are published or not. The documents may come from teaching and research institutions in France or abroad, or from public or private research centers.

L'archive ouverte pluridisciplinaire **HAL**, est destinée au dépôt et à la diffusion de documents scientifiques de niveau recherche, publiés ou non, émanant des établissements d'enseignement et de recherche français ou étrangers, des laboratoires publics ou privés.

Gonadotropin-Releasing Hormone Stimulates the Biosynthesis of Pregnenolone Sulfate and Dehydroepiandrosterone Sulfate in the Hypothalamus

Delphine Burel,* Jian Hua Li,* Jean-Luc Do-Rego, Ai Fen Wang, Van Luu-The, Georges Pelletier, Yves Tillet, Catherine Taragnat, Hyuk Bang Kwon, Jae Young Seong, and Hubert Vaudry

Laboratory of Neuronal and Neuroendocrine Differentiation and Communication (D.B., J.-L.D.-R., H.V.), Institut National de la Santé et de la Recherche Médicale U982, Research Institute for Biomedicine (IRIB), International Associated Laboratory Samuel de Champlain, University of Rouen, 76821 Mont-Saint Aignan, France; Hormone Research Center (J.H.L., A.F.W., H.B.K.), Chonnam National University, Gwangju 500-757, Korea; Research Center in Molecular Endocrinology, Oncology and Genetics (V.L.T., G.P., H.V.), Laval University Hospital Center, Québec, Ontario, G1V4G2, Canada; Laboratory of Reproductive Physiology and Behaviors (Y.T., C.T.), Unité Mixte de Recherche MR 6175 Institut National de la Recherche Agronomique-Centre National de la Recherche Scientifique, University of Tours-Haras Nationaux, 37380 Nouzilly, France; and Laboratory of G-Protein-Coupled Receptors (J.Y.S.), Graduate School of Medicine, Korea University, Seoul 136-705, Korea

The sulfated neurosteroids pregnenolone sulfate (Δ^5 PS) and dehydroepiandrosterone sulfate (DHEAS) are known to play a role in the control of reproductive behavior. In the frog *Pelophylax ridibundus*, the enzyme hydroxysteroid sulfotransferase (HST), responsible for the biosynthesis of Δ^5 PS and DHEAS, is expressed in the magnocellular nucleus and the anterior preoptic area, two hypothalamic regions that are richly innervated by GnRH1-containing fibers. This observation suggests that GnRH1 may regulate the formation of sulfated neurosteroids to control sexual activity. Double labeling of frog brain slices with HST and GnRH1 antibodies revealed that GnRH1-immunoreactive fibers are located in close vicinity of HST-positive neurons. The cDNAs encoding 3 GnRH receptors (designated riGnRHR-1, -2, and -3) were cloned from the frog brain. RT-PCR analyses revealed that riGnRHR-1 is strongly expressed in the hypothalamus and the pituitary whereas riGnRHR-2 and -3 are primarily expressed in the brain. In situ hybridization histochemistry indicated that GnRHR-1 and GnRHR-3 mRNAs are particularly abundant in preoptic area and magnocellular nucleus whereas the concentration of GnRHR-2 mRNA in these 2 nuclei is much lower. Pulse-chase experiments using tritiated Δ^5 P and DHEA as steroid precursors, and 3'-phosphoadenosine 5'-phosphosulfate as a sulfonate moiety donor, showed that GnRH1 stimulates, in a dose-dependent manner, the biosynthesis of Δ^5 PS and DHEAS in frog diencephalic explants. Because Δ^5 PS and DHEAS, like GnRH, stimulate sexual activity, our data strongly suggest that some of the behavioral effects of GnRH could be mediated via the modulation of sulfated neurosteroid production. (*Endocrinology* 154: 2114–2128, 2013)

The two sulfated neurosteroids pregnenolone sulfate (Δ^5 PS) and dehydroepiandrosterone sulfate (DHEAS) are known to play a major role in the regulation of neurophysiological and behavioral processes (for reviews, see

Refs. 1–3). Specifically, Δ^5 PS is implicated in long-term potentiation (4), learning (5), and cognition (6) whereas DHEAS exerts various neuroprotective effects (7, 8), improves memory deficits after brain injury (9), and de-

ISSN Print 0013-7227 ISSN Online 1945-7170
Printed in U.S.A.

Copyright © 2013 by The Endocrine Society

Received January 25, 2013. Accepted March 28, 2013.

First Published Online April 3, 2013

* D.B. and J.H.L. contributed equally to this study.

Abbreviations: CNS, central nervous system; DAR, donkey antirabbit; DAS, donkey anti-sheep; DHEA, dehydroepiandrosterone; DHEAS, dehydroepiandrosterone sulfate; ES, estrone sulfate; GnRHR, GnRH receptor; HST, hydroxysteroid sulfotransferase; Mgd, dorsal magnocellular nucleus; NPY, neuropeptide Y; PAPS, 3'-phosphoadenosine 5'-phosphosulfate; Poa, preoptic area; Δ^5 PS, pregnenolone sulfate; SSC, saline sodium citrate; THF, tetrahydrofuran; TM, transmembrane.

creases the nociceptive threshold in mice (10). The synthesis of these sulfated 3-hydroxysteroids is catalyzed by a cytosolic enzyme termed hydroxysteroid sulfotransferase (HST), which transfers the sulfonate moiety from the donor molecule 3'-phosphoadenosine 5'-phosphosulfate (PAPS) onto the 3-hydroxy acceptor site of pregnenolone (Δ^5 P) and dehydroepiandrosterone (DHEA). In mammals, the occurrence of HST in the central nervous system (CNS) and the biosynthesis of sulfated steroids in situ in the brain are currently a matter of debate. Although early studies had shown the presence of high amounts of Δ^5 PS and DHEAS (11–13) and HST activity (14, 15) in the brain, more recent reports, based on specific ELISA techniques and nano-HPLC/mass spectroscopy analytical methods, have cast doubt on the presence of Δ^5 PS and DHEAS in the brain of rodents (16–19). In agreement with these latter reports, attempts to localize HST in the rat brain have been unsuccessful (20).

In contrast, the amphibian brain represents a very suitable model in which to investigate the regulation of sulfated neurosteroid biosynthesis. First, the distribution and biologic activity of HST have been studied in detail in the frog CNS (21–23). Second, the rate of biosynthesis of sulfated neurosteroids in the frog brain is so high that it is possible to investigate the mode of action of inhibitory neurotransmitters or neuropeptides on HST-expressing neurons. Thus, it has been demonstrated that neuropeptide Y (NPY), acting through Y1 receptors, inhibits the biosynthesis of Δ^5 PS and DHEAS by frog hypothalamic explants (24). These data indicate that the frog brain has the capability of synthesizing sulfated neurosteroids and that the activity of HST is finely tuned by regulatory neuropeptides.

GnRH has been initially isolated from the mammalian hypothalamus on the basis of its ability to stimulate gonadotropin biosynthesis and secretion (25, 26). In most vertebrates, at least 2, and usually 3, molecular forms of GnRH appear to coexist in each single species: 1) a species-specific form generally termed GnRH1; 2) an evolutionary-conserved form that has been first isolated from the chicken brain and thus termed chicken GnRH2 and now referred to as GnRH2; and 3) a salmon GnRH form designated GnRH3 (for review see Ref. 27). In the frog *Rana ridibunda*, now renamed *Pelophylax ridibundus* (28), the two GnRH isoforms correspond to mammalian GnRH (GnRH1) and chicken GnRH2 (GnRH2) (29). Neurons expressing GnRH1, which are restricted to the anterior preoptic area (Poa), project through the ventral diencephalon toward the median eminence, whereas neurons expressing GnRH2 are widely distributed throughout the frog brain (30). GnRHs exert their action through interaction with GnRH receptors (GnRHRs) that belong to the

G protein-coupled receptor family. GnRHRs have now been cloned in a number of species from fish to human (27). Thus, 4 or 5 isoforms have been characterized in teleost fish (31, 32) whereas 2 types of GnRHRs have been identified in monkey (33) and 3 forms in frog (34, 35).

Interestingly, HST, the enzyme responsible for the biosynthesis of sulfated neurosteroids, is expressed in frog brain regions that are richly innervated by GnRH1-containing fibers, notably in the dorsal magnocellular nucleus (Mgd) and Poa (21, 30). Moreover, sulfated neurosteroids, in very much the same manner as GnRH, are implicated in the control of sexual behavior in various vertebrates (36–38). Finally, it has been demonstrated that, in frog, the amount of Δ^5 PS in the brain increases during the breeding period and decreases during hibernation (39). These observations suggest that GnRH1 and sulfated neurosteroids may interact to regulate reproductive function in amphibians. In the present study, we have thus investigated the distribution of the 3 mRNAs encoding GnRHRs in the brain of the European green frog *Pelophylax ridibundus*, and we have studied the possible implication of GnRH1 in the regulation of HST activity.

Materials and Methods

Animals

Adult male frogs (*Pelophylax ridibundus*; body weight 30–40 g) were purchased from a commercial supplier (Coué-tard, St-Hilaire de Riez, France). The animals were housed in a temperature-controlled room ($8 \pm 0.5^\circ\text{C}$) under running water, on a 12-hour dark, 12-hour light regimen (lights on from 6:00 AM to 6:00 PM), for at least 1 week before use. In order to limit possible variations due to circadian rhythms (40), all animals were killed between 9:30 AM and 10:30 AM. Animal manipulations were performed according to the recommendations of the French Ethical Committee and under the supervision of authorized investigators.

Antibodies, chemicals, and plasmids

The antiserum against sulfotransferase was raised by immunizing rabbits with a synthetic peptide corresponding to the sequence 180–192 of rat liver HST (41). This antiserum has been used previously to localize HST-immunoreactive neurons in the frog brain (21, 24). The antiserum against GnRH1 was raised in sheep (42). Texas Red-conjugated donkey antirabbit (DAR) γ -globulins were supplied by GE Healthcare Europe GmbH (Velizy-Villacoublay, France). Alexa 488-conjugated donkey anti-sheep γ -globulins (DAS/Alexa 488) were from Invitrogen (Cergy Pontoise, France).

Testosterone sulfate (TS) and estrone sulfate (ES) were purchased from Steraloids, Inc (Newport, Rhode Island). Δ^5 P, Δ^5 PS, DHEA, DHEAS, 3-aminobenzoic acid ethyl ester (MS 222), and GnRH1 were supplied by Sigma (St Louis, Missouri). Tritiated Δ^5 P (7-[^3H] Δ^5 P; 21 Ci/mmol), tritiated DHEA (1,2,6,7-[^3H]DHEA; 60 Ci/mmol), and ^{35}S -labeled PAPS (3'-[^{35}S]PAPS; 1.13

Ci/mmol) were obtained from Du Pont-New England Nuclear (Les Ulis, France). Propylene glycol, HEPES, dichloromethane, hexane, and tetrahydrofuran (THF) were from Sigma-Aldrich (Saint Quentin Fallavier, France). BSA (Fraction V) was from Boehringer (Mannheim, Germany).

The pcDNA3 expression vector was purchased from Invitrogen (Carlsbad, California). The pCMV β -Gal plasmid was purchased from CLONTECH Laboratories, Inc (Palo Alto, California). The CRE-luc vector that contains 4 copies of the cAMP response element (CRE, TGACGTCA) was obtained from Stratagene (La Jolla, California). The c-fos-luc vector containing the -711 ~ +45 sequence of the human c-fos promoter constructed in the pFLASH vector, was a kind gift from Dr R. Prywes (Columbia University, New York, New York).

Isolation of GnRHR cDNAs

Total RNA was extracted from pituitary and brain by Trizol agent (Sigma). The first strand of cDNA was synthesized by using 1 μ g of total RNA, oligo-dT primer, and SuperScript II Ribonuclease H⁻ reverse transcriptase (Life Technologies, Gaithersburg, Maryland). The sequences of the specific primers from *Rana dybowskii* (35) used to amplify the cDNAs encoding GnRHR open reading frames in *Pelophylax ridibundus* (designated riGnRHR) are indicated in Supplemental Table 1 published on The Endocrine Society's Journals Online web site at <http://endo.endojournals.org>.

To amplify the full-length open reading frame of each riGnRHR, Vent DNA Taq polymerase (New England Biolabs, Herts, United Kingdom) was used. PCR conditions were set as follows: denaturation at 95 °C for 4 minutes, followed by 32 cycles at 94°C for 20 seconds, at 55°C for 30 seconds, and at 72°C for 2 minutes. PCR products of the expected size were excised, purified, and cloned into the *EcoRI* and *XbaI* sites of pcDNA3 (Invitrogen), generating pc-riGnRHR-1, pc-riGnRHR-2, and pc-riGnRHR-3. Positive clones were isolated and purified using a QIAGEN plasmid Mini kit (QIAGEN, Chatsworth, California). DNA sequences were confirmed by the dideoxy chain termination method using a Sequenase Version 2 kit (USB Corp, Cleveland, Ohio) or the Dye Terminator Cycle Sequencing Ready Reaction Kit (Perkin-Elmer, Boston, Massachusetts).

RT-PCR analysis

One microgram of total RNA prepared from various tissues was reverse-transcribed and 1 μ l of 20 μ l was subjected to PCR. Because there are 2 introns located in the transmembrane domain (TM) IV and between TMV and TM VI (33, 43-45), primers that span at least 1 intron were employed to avoid genomic contamination. The sequences of these primers are indicated in Supplemental Table 1.

The PCR conditions were set as follows: denaturation at 95°C for 30 seconds, followed by 32 cycles (37 for riGnRHR-2) at 94°C for 20 seconds, 58°C for 30 seconds, and 72°C for 30 seconds. The PCR products were separated by agarose gel followed by ethidium bromide staining. Internal controls were performed as previously described (46).

Cell culture, transient transfection, and luciferase assay

CV-1 cells were maintained at 37°C in DMEM with 10% heat-inactivated fetal bovine serum, 1 mM glutamate, 100 U

penicillin, and 100 μ g/mL streptomycin. Cells were cultured in 24-well plates, and transfection was performed using the SuperFect transfection kit (QIAGEN) according to the manufacturer's instructions. For each transfection, 100 ng of each receptor cDNA, and 200 ng of CRE-luc or c-fos-luc vector along with 200 ng of internal control plasmid pCMV β -Gal were used. One day after transfection, cells were serum starved for 24 hours and then challenged with GnRH1 and GnRH2 for 6 hours. Cells were harvested, and the luciferase activity in the cell extract was determined according to standard methods in a Lumat LB9501 (EG & G Berthold, Bad Wildbad, Germany). Luciferase activities were normalized using β -galactosidase values. Transfection experiments were performed in duplicate and repeated 3 to 5 times. The GnRH concentrations inducing half-maximal stimulation (EC₅₀) were calculated using the PRISM2 software (GraphPad Software, Inc., San Diego, California).

Riboprobe synthesis

The cDNA fragments containing the sequences 888~1224 for riGnRHR-1, 660~1110 for riGnRHR-2, and 933~1275 for riGnRHR-3 were amplified and cloned into the pGEMT easy vector (Promega Corp, Madison, Wisconsin). The plasmid pGEM-T containing riGnRHR-1, riGnRHR-2, or riGnRHR-3 cDNA was linearized with *Sall* or *NcoI* to synthesize sense or antisense riboprobes, respectively. Four hundred nanograms of the linearized plasmid was incubated at 37°C for 1 hour in a solution containing transcription buffer, ATP, CTP, GTP (1 mM each), 140 μ Ci ³⁵S-UTP (Amersham Pharmacia Biotech, Buckinghamshire, UK), RNase inhibitor, and 2.5 U of the appropriate RNA polymerase (Roche Molecular Biochemicals, Mannheim, Germany). The DNA template was digested by 5 U DNase at 37°C for 15 minutes. The probe was extracted by phenol/chloroform. The supernatant was further purified on a Sephadex G50 column equilibrated with loading buffer (0.1% sodium dodecyl sulfate, 10 mM Tris-HCl, pH 7.5, EDTA 1 mM). The radioactivity of the fraction was determined in a β -counter.

In situ hybridization

In situ hybridization was performed as previously described (47). Briefly, adult frogs were anesthetized by immersion in 0.1% MS 222 and perfused transcardially with 4% paraformaldehyde. Brain sections were cut at 12 μ m in the frontal plane in a cryomicrotome (Frigocut 2700, Leica, Nussloch, Germany) and mounted on poly-L-lysine- and gelatin-coated slides. Sections were incubated for 10 minutes in 0.1 M triethanolamine/0.9% NaCl (pH 8.0)/0.25 acetic anhydride, rinsed in 2 \times saline sodium citrate (SSC), and covered for 60 minutes with prehybridization buffer (pH 7.5) containing 50% formamide, 0.6 M NaCl, 10 mM Tris-HCl (pH 7.5), 1 \times Denhart, 1 mM EDTA (pH 8.0), 550 μ g/mL denatured salmon sperm DNA, and 50 μ g/mL yeast tRNA. Hybridization was performed overnight at 50°C in the same buffer (except for salmon sperm DNA, the concentration of which was lowered to 60 μ g/mL) supplemented with 10 mM dithiothreitol, 10% dextran sulfate, and 1.5 \times 10⁷ cpm/mL heat-denatured RNA sense or antisense riboprobes. Slices were then washed in 2 \times SSC at 50°C and treated with ribonuclease A (50 μ g/mL) at 37°C for 60 minutes. High-stringency washes were performed at 55 °C in 0.01 \times SSC containing 14 mM β -mercaptoethanol and 0.05% sodium pyrophosphate. The tissue sections were dehydrated in ethanol and exposed onto Biomax MR Film

(Eastman Kodak, Rochester, New York) for 1 week. Tissue slices were subsequently dipped into an NTB2 (Kodak) liquid emulsion at 42°C, exposed for 2 months and developed. To identify anatomic structures, the sections were stained with hematoxylin/eosin and observed with a Zeiss microscope (Axioskop 2) using Magna Fire SP (Optronics, Goleta, California).

Immunofluorescence procedure

Frogs were anesthetized and perfused transcardially with 50 mL of 0.1 M PBS (pH 7.4). The perfusion was carried on with 50 mL of Bouin's fixative, cryoprotected and frozen at -80°C. Brain sections were cut at 7 μ m in the frontal or sagittal plane in a cryomicrotome. Tissue sections were incubated overnight at 4°C in a humid atmosphere with both HST (1:100) and GnRH1 (1:500) antisera diluted in PBS containing 0.3% Triton X-100 and 1% BSA. The sections were then rinsed for 1 hour in PBS, and incubated for 1.5 hours at room temperature with DAR/Texas Red and DAS/Alexa 488 (10 μ g/mL each). Finally, the sections were rinsed for 1 hour in PBS and mounted with PBS/glycerol (vol/vol) before examination under a confocal laser scanning microscope (CLSM, Leica). To study the specificity of the immunoreaction, the following controls were performed: 1) substitution of the HST or GnRH antiserum with PBS; 2) incubation with nonimmune rabbit serum; 3) preincubation of the HST antiserum with the synthetic peptide hapten (5×10^{-6} M); and 4) preincubation of the GnRH antiserum with graded concentrations of synthetic GnRH1 or GnRH2 (10^{-9} to 10^{-4} M). Neuroanatomic nomenclature was based on the atlas of Neary and Northcutt (48).

Measurement of HST activity

For each experiment, 5 frog hypothalami were rapidly dissected, sliced, and preincubated at 24°C for 30 minutes in the presence of [35 S]PAPS (4.5×10^{-6} M) diluted in 1 mL of Ringer's solution consisting of 15 mM HEPES, 112 mM NaCl, 15 mM NaHCO₃, 2 mM CaCl₂, and 2 mM KCl, supplemented with 2 mg of glucose/mL and 0.3 mg of BSA/mL. The incubation medium was gassed with a 95% O₂/5% CO₂ mixture and the pH was adjusted to 7.4. Hypothalamic slices were then incubated at 24°C for 2 hours in 500 μ L of Ringer's medium containing 10^{-6} M [3 H] Δ^5 P or 10^{-7} M [3 H]DHEA, 4.5×10^{-6} M [35 S]PAPS, and 4% propylene glycol, in the absence or presence of graded concentrations of GnRH1 (10^{-8} to 10^{-5} M). At the end of the incubation period, the medium was removed, the reaction was stopped by adding 1 mL of ice-cold Ringer's medium, and the tissues were homogenized. Sulfated and unconjugated steroids were extracted 3 times with 1 mL of dichloromethane (21). The aqueous phase containing sulfated steroids was evaporated in a Speed Vac concentrator (Savant, Hicksville, New York), and the dry extract was prepurified on a Sep-Pak C₁₈ cartridge (Waters Associates, Milford, Massachusetts) equilibrated with hexane. Sulfated steroids were eluted with 3 mL of a solution made of 70% hexane and 30% THF. The solvent was evaporated in a Speed Vac concentrator, and the dry extract was kept at 4°C until HPLC analysis.

HPLC

Sep-Pak-prepurified diencephalic extracts were analyzed by reversed-phase HPLC on a Gilson liquid chromatograph (Unipoint System, Villiers-le-Bel, France) equipped with a 0.39 \times

30-cm Nova-Pak C₁₈ column (Waters Associates) equilibrated with 100% hexane. Radioactive steroids were eluted at a flow rate of 1 mL/min using a gradient of THF (0%-100% over 45 min) including three isocratic steps at 0% (0-10 min), 2% (15-20 min), and 100% (35-45 min). Fractions were collected at 0.5-minute intervals. A 400- μ L aliquot of each HPLC fraction was mixed with 4 mL of liquid scintillator (Aquasafe 300 Plus, Zimer Analytic, Frankfurt, Germany) and counted in a double-channel liquid scintillation counter (1211 Minibeta, LKB Wallac, Gaithersburg, Maryland) using the specific windows for 3 H and 35 S. Synthetic steroids used as reference standards were chromatographed under the same conditions as the tissue extracts, and their elution position was determined by ultraviolet (UV) absorption.

Quantification of steroid biosynthesis and statistical analysis

The amounts of radioactive sulfated steroids formed by conversion of [3 H] Δ^5 P or [3 H]DHEA were expressed as a percentage of the total radioactivity contained in all peaks resolved by HPLC, including [3 H] Δ^5 P or [3 H]DHEA for the 3 H-labeled neosynthesized steroids, or including [35 S]PAPS for the 35 S-labeled neosynthesized steroids. Each value is the mean of 3 independent experiments. Statistical significance was determined using unpaired *t* test, and comparisons among groups were performed by ANOVA, with post hoc Tukey's test using the InStat version 3.01 program (GraphPad Inc).

Results

Isolation of three types of GnRHR from *Pelophylax ridibundus*

Sequence analysis of the open reading frame of each riGnRHR cDNA revealed that riGnRHR-1, riGnRHR-2, and riGnRHR-3 encode 407-, 371-, and 424-amino acid proteins, respectively. These sequence data have been submitted to the GenBank databases under accession number AY260153 for riGnRHR-1, AY260154 for riGnRHR-2, and AY260155 for riGnRHR-3. All 3 riGnRHRs showed typical characteristics of G protein-coupled receptors, such as 7 hydrophobic TM domains, N-terminal and C-terminal tails (Figure 1). The percentages of amino acid sequence identity between riGnRHRs and GnRHRs from various vertebrate species are indicated in Table 1. RiGnRHR-1 shares 95% identity with bullfrog *Rana catesbeiana* GnRHR-1 whereas riGnRHR-2 and riGnRHR-3 share 96% identity with bullfrog GnRHR-2 and bullfrog GnRHR-3, respectively. Moreover, riGnRHR-2 shows high sequence identity with chicken GnRHR (57%), followed by fish GnRHRs (49%-50%), monkey GnRHR-2 (39%-40%), and rat GnRHRs (35%) whereas riGnRHR-1 and riGnRHR-3 have the highest homology with monkey GnRHR-2 (43%-46%), followed by chicken GnRHR (40%-43%), fish GnRHRs (39%), and rat type-I GnRHR (31%-33%) (Table 1). However, the de-

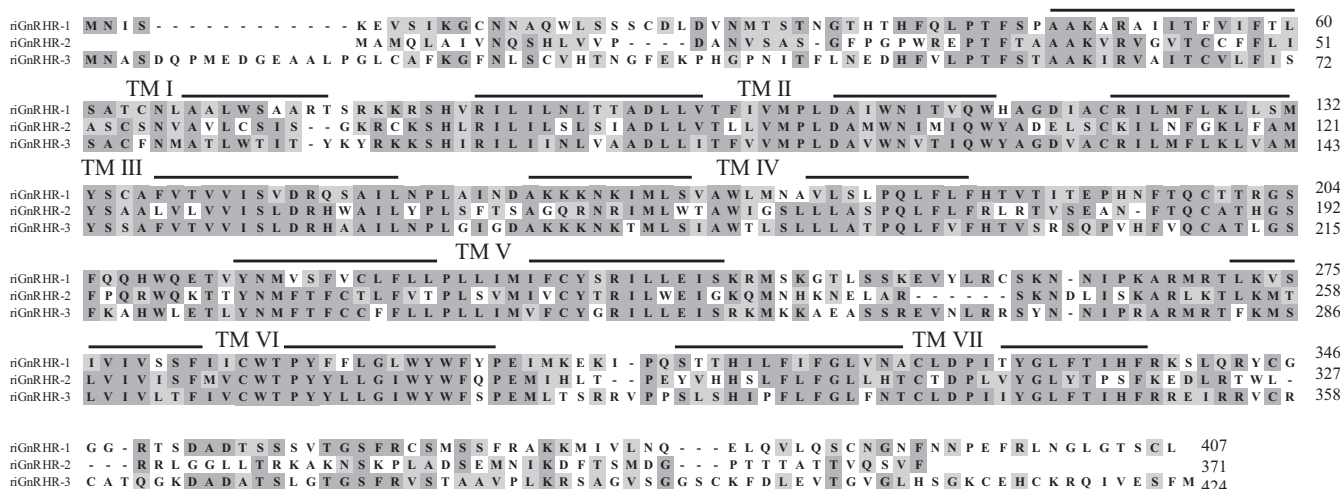


Figure 1. Alignment of Amino Acid Sequences of riGnRHRs. Identical amino acids are shaded. Amino acid numbers are indicated on the right. Gaps introduced for optimal alignment are indicated as dashes. The predicted TM domains are indicated on the top of the sequences. riGnRHR-1, *Pelophylax ridibundus* type I GnRHR; riGnRHR-2, *P. ridibundus* type II GnRHR; riGnRHR-3, *P. ridibundus* type III GnRHR.

degree of sequence homology among riGnRHRs is relatively low. Thus, riGnRHR-1 shows 51% and 39% identity with riGnRHR-3 and riGnRHR-2, respectively, and riGnRHR-3 shows 40% identity with both riGnRHR-1 and riGnRHR-2.

Ligand specificity and signal transduction of riGnRHRs

The effects of the 2 native GnRH forms, GnRH1 and GnRH2, on CV-1 cells transfected with plasmids containing each riGnRHR were studied using the CRE-luc or c-fos-luc reporter systems. Both GnRH1 and GnRH2 significantly increased luciferase activity in either CRE-luc or c-fos-luc-cotransfected cells. In cells expressing riGnRHR-1 and riGnRHR-3, GnRHs induced 2~3 fold higher c-fos promoter-driven luciferase activity than CRE-driven luciferase activity. In cells expressing riGnRHR-2, GnRHs induced CRE- and c-fos promoter-driven luciferase activity with similar strength. Regarding ligand sensitivity, riGnRHR-1 was slightly more sensitive to GnRH2 than

GnRH1 in both CRE-luc and c-fos-luc assay systems. For riGnRH-2 and riGnRH-3, GnRH2 was 447 times and 74 times more potent than GnRH1 in the c-fos-luc assay system, and 776 times and 40 times more potent than GnRH1 in the CRE-luc reporter system, respectively (Figure 2 and Supplemental Table 2).

Tissue expression of the 3 riGnRHR mRNAs

To examine the tissue distribution of each riGnRHR, RT-PCR was performed by using total RNAs isolated from olfactory lobe, telencephalon, hypothalamus, mesencephalon, cerebellum, rhombencephalon, spinal cord, distal lobe and neurointermediate lobe of the pituitary, testis, liver, kidney, adrenal gland, and lung. Because there are two introns located in TM IV and at the border between TM V and TM VI (33, 43–45), primers that span 2 introns were employed. As shown in Supplemental Figure 1, the 3 riGnRHR mRNAs were amplified in all brain regions as well as in the testis. In contrast, GnRHR-1 mRNA was selectively expressed in the distal lobe of the

Table 1. Amino Acid Identity among GnRHRs

| | riGnRHR-1 (%) | RiGnRHR-2 (%) | riGnRHR-3 (%) |
|----------------------|---------------|---------------|---------------|
| Human GnRHR | 32 | 35 | 31 |
| Rat GnRHR-1 | 33 | 35 | 32 |
| Marmoset GnRHR-2 | 43 | 40 | 45 |
| Green monkey GnRHR-2 | 43 | 39 | 46 |
| Goldfish GnRHR-1A | 39 | 50 | 39 |
| Goldfish GnRHR-1B | 39 | 49 | 39 |
| Chicken GnRHR | 43 | 57 | 40 |
| Bullfrog GnRHR-1 | 95 | 38 | 52 |
| Bullfrog GnRHR-2 | 38 | 96 | 39 |
| Bullfrog GnRHR-3 | 52 | 39 | 96 |

Amino acid identity was determined using the CLUSTAL W(1.4) alignment program.

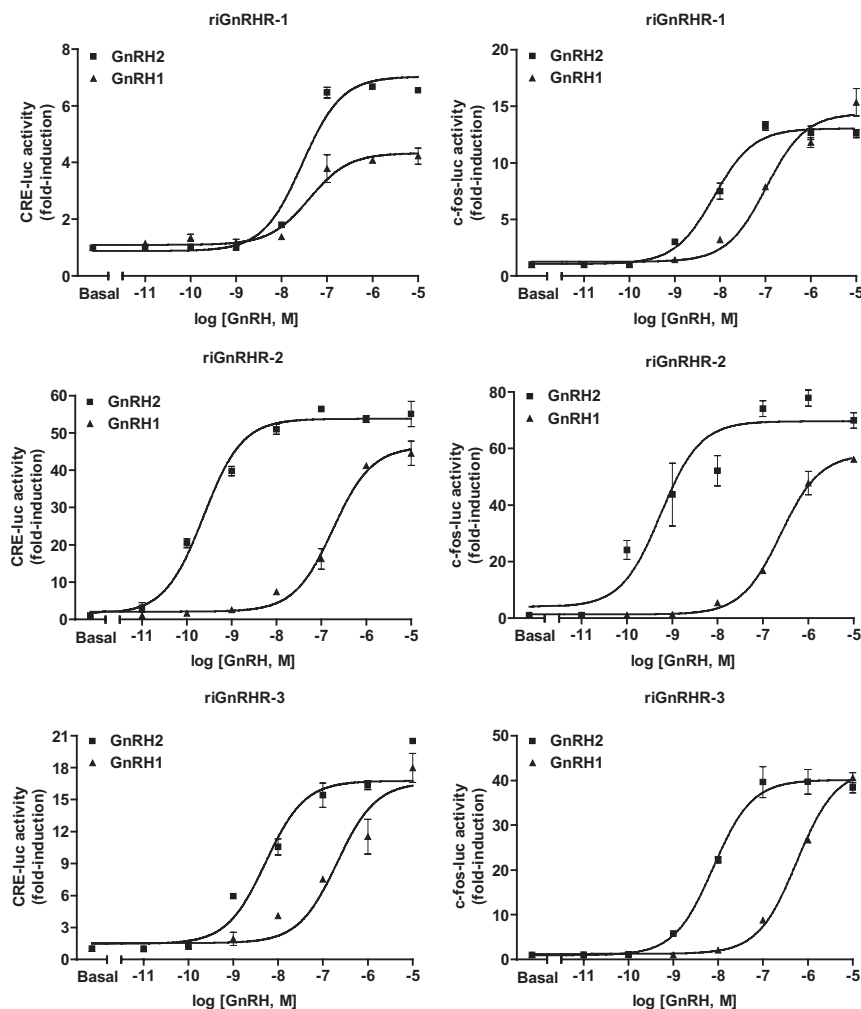


Figure 2. CRE- and c-fos-Promoter Driven Transcriptional Activity of riGnRHRs. CV-1 cells were cotransfected with 100 ng of each receptor construct and 200 ng of c-fos-luc or CRE-luc reporter plus 100 ng pCMV β -gal plasmid. After 24 hours of transfection, cells were serum starved for 24 hours and then incubated with graded concentrations of GnRH1 (\blacktriangle) or GnRH2 (\blacksquare) for 6 hours. Cells were lysed and subjected to luciferase assay. Data were normalized over basal activity.

pituitary whereas GnRHR-2 and GnRHR-3 mRNAs were detected only in the adrenal gland and the liver, respectively (Supplemental Figure 1).

Brain distribution of the 3 riGnRHR mRNAs

The distribution of each riGnRHR mRNA in the frog brain was determined by *in situ* hybridization. The results are summarized in Table 2. In the telencephalon, strong hybridization signals for riGnRHR-1 and -3 mRNAs were observed in the pallium, the septum, and the striatum (Figure 3A). Moderate signals for riGnRHR-1 and -3 mRNAs were seen in the internal granular layer and the nucleus accumbens. Weak to moderate signals for riGnRHR-2 mRNA were detected in the postolfactory eminence, the lateral pallium, the dorsal pallium, and the nucleus accumbens. Other regions, such as the accessory olfactory bulb, the vomeronasal nerve, and the entopeduncular nucleus, were totally devoid of signal.

In the diencephalon, intense labeling for riGnRHR-1 and -3 mRNA was seen in Poa (Figure 3B). Caudally, both riGnRHR-1 and -3 mRNAs were found in the magnocellular preoptic nucleus, the organum vasculosum, the suprachiasmatic nucleus, the hypothalamic nucleus, the posterior tuberculum, the nucleus of the periventricular organ, and the habenular nucleus. The ventrolateral, anterior, central, and posterior thalamic nuclei also expressed both riGnRHR-1 and -3 mRNAs. mRNA for riGnRHR-3, but not riGnRHR-1, was detected in the lateral amygdala (Figure 3C). No signal for riGnRHR-1 and -3 was observed in the lateral thalamic nucleus, the subcommissural organ, the uncinate neuropil, or the optic chiasma. Only the ventral part of the magnocellular preoptic nucleus and the posterior thalamic nucleus expressed riGnRHR-2 mRNA (Figure 3B).

In the mesencephalon, the optic tectum, the tectal lamina six, and the nucleus of the medial longitudinal fasciculus were intensely labeled by the 3 riGnRHR probes (Figure 3D). The pretectal gray and the pretoral gray were also labeled by the 3 probes although with variable intensity (Figure 3D). riGnRHR-1 and -3

mRNA signals were seen throughout the tegmental nucleus (Figure 3D). The nucleus reticularis isthmi expressed only riGnRHR-1 mRNA (Figure 3D), whereas the nucleus cerebelli expressed only riGnRHR-3 mRNA. No hybridization signal was detected in the nucleus of the posterior commissure, the nucleus of the lentiformis mesencephali, the nucleus interpeduncularis, and the nucleus isthmi.

In the metencephalon, weak hybridization signals for riGnRHR-1 and -3 mRNAs were seen in the cerebellar region, whereas no positive signal for riGnRHR-2 mRNA was detected in this region. In the rhombencephalon, moderate to strong signals for the three receptor mRNAs were observed in the nucleus of the trigeminal nerve, the nucleus of the abducent nerve, the nucleus of the facial nerve, the nucleus of the stato-acusticus nerve, and the sulcus limitans (Figure 3E). Faint signal for riGnRHR-1 mRNA was also detected in the fasciculus solitarius.

Table 2. Comparative Localization and Relative Abundance of the 3 Types of riGnRHR mRNAs in the Brain

| Structure | riGnRHR-1 | riGnRHR-2 | riGnRHR-3 |
|---|-----------|-----------|-----------|
| Telencephalon | | | |
| Olfactory bulb, internal granular layer (IGL) | + | – | + |
| Olfactory bulb, extragranular plexiform layer (EPL) | – | – | – |
| Olfactory bulb, mitral cellular layer (ML) | – | – | – |
| Olfactory bulb, glomerular layer (GL) | – | – | – |
| Accessory olfactory bulb (AOB) | – | – | – |
| Vomerolateral nerve (VN) | – | – | – |
| Postolfactory eminence (PE) | ++ | ± | + |
| Lateral pallidum (LP) | +++ | + | +++ |
| Dorsal pallidum (DP) | +++ | + | +++ |
| Medial pallidum (MP) | +++ | + | +++ |
| Lateral septum (LS) | ++ | ± | ++ |
| Ventral striatum (Vst) | | | |
| Dorsal striatum (Dst) | +++ | ± | +++ |
| Nucleus of the diagonal band of Broca (NDB) | + | – | ± |
| Nucleus accumbens (NA) | ++ | + | +++ |
| Medial amygdala (MA) | ++ | – | +++ |
| Medial septum (MS) | ++ | + | ++ |
| Lateral amygdala (LA) | – | – | ++ |
| Anterior entopeduncular nucleus (Ea) | – | – | – |
| Posterior entopeduncular nucleus (Ep) | – | – | – |
| Bed nucleus of the pallidum commissure (BN) | – | – | + |
| Diencephalon | | | |
| Anterior preoptic area (Poa) | +++ | ± | +++ |
| Magnocellular preoptic nucleus, dorsal part (Mgd) | ++ | + | +++ |
| Magnocellular preoptic nucleus, ventral part (Mgv) | ++ | + | +++ |
| Organum vasculosum (OV) | ++ | ± | ++ |
| Suprachiasmatic nucleus (SC) | +++ | – | +++ |
| Dorsal hypothalamic nucleus (DH) | + | – | ++ |
| Ventral hypothalamic nucleus (VH) | ++ | – | +++ |
| Lateral hypothalamic nucleus (LH) | – | – | – |
| Posterior tuberculum (TP) | ++ | – | ++ |
| Nucleus of the periventricular organ (NPv) | | | |
| Epiphysis (E) | – | – | – |
| Thalamic eminence (TE) | – | – | – |
| Habenular commissure (Hc) | ++ | – | ++ |
| Dorsal habenular nucleus (Hd) | ++ | – | ++ |
| Ventral habenular nucleus (Hv) | ++ | + | ++ |
| Bed nucleus of the stria medullaris (BM) | – | – | + |
| Neuropil of Bellonci (B) | – | – | – |
| Nucleus of Bellonci (NB) | + | – | – |
| Ventrolateral thalamic nucleus, dorsal part (Vld) | ++ | – | – |
| Ventrolateral thalamic nucleus, ventral part (Vlv) | ++ | – | ++ |

(Continued)

Table 2. Continued

| Structure | riGnRHR-1 | riGnRHR-2 | riGnRHR-3 |
|---|-----------|-----------|-----------|
| Ventromedial thalamic nucleus (VM) | + | + | + + |
| Anterior thalamic nucleus (A) | + | — | + + |
| Superficial ventral thalamic nucleus (Vs) | — | — | + |
| Corpus geniculatum thalamicum (CP) | — | — | — |
| Lateral thalamic nucleus, anterior division (La) | ± | — | — |
| Lateral thalamic nucleus, posterodorsal division (Lpd) | — | — | — |
| Lateral thalamic nucleus, posteroventral division (Lpv) | — | — | — |
| Central thalamic nucleus (CNT) | + | — | + + |
| Posterior thalamic nucleus (P) | + + | + | + + |
| Subcommissural organ (CO) | — | — | — |
| Uncinate neuropil (U) | — | — | — |
| Optic chiasma (OC) | — | — | — |
| Optic nerve (ON) | — | — | — |
| Mesencephalon | | | |
| Optic tectum (OT) | + + + | + + | + + |
| Tectal lamina six (6) | + + | + | + + |
| Nucleus of the posterior commissure (NPC) | — | — | — |
| Nucleus lentiformis mesencephali (NLM) | — | — | — |
| Nucleus of the medial longitudinal fasciculus (NMLF) | + + + | + + | + + + |
| Basic optic nucleus (BON) | + | — | — |
| Nucleus profundus mesencephali (NPM) | + | — | — |
| Pretectal gray (PtG) | + | ± | ± |
| Pretoral gray (PtrG) | + + | ± | ± |
| Oculomotor and trochlear nuclei (III) | + + + | + + | + + |
| Torus semicircularis (TS) | + + + | + | + + |
| Anterodorsal tegmental nucleus (AD) | + + + | + | + + |
| Anteroventral tegmental nucleus (AV) | + + + | + | + + |
| Posterodorsal tegmental nucleus (PD) | + | — | + + |
| Posteroventral tegmental nucleus (PV) | + | — | + |
| Nucleus reticularis isthmi (RIS) | + | — | — |
| Nucleus interpeduncularis (NIP) | — | — | — |
| Nucleus isthmi (NI) | — | — | — |
| Nucleus cerebelli (Cer) | — | — | + + |
| Metencephalon | | | |
| Molecular cell layer of the cerebellum (MC) | — | — | — |
| Purkinje cell layer of the cerebellum (PC) | ± | — | — |
| Granular cell layer of the cerebellum (GC) | + | — | ± |
| Auricular lobe of the cerebellum (CAL) | — | — | — |

(Continued)

Table 2. Continued

| Structure | riGnRHR-1 | riGnRHR-2 | riGnRHR-3 |
|---|-----------|-----------|-----------|
| Rhombencephalon | | | |
| Choroid plexus (Pch) | – | – | – |
| Sulcus limitans (SL) | + + | ± | + + |
| Griseum central rhombencephali (Gc) | – | – | – |
| Raphe nucleus (Ra) | – | – | – |
| Nucleus reticularis inferior (Ri) | – | – | – |
| Nucleus reticularis medius (Rm) | – | – | – |
| Fasciculus solitarius (FS) | ± | – | – |
| Nucleus of the trigeminal nerve (V) | + | + | + |
| Nucleus of the abducent nerve (VI) | + + | + | + + |
| Nucleus of the facial nerve (VII) | + + | + | + + |
| Dorsal nucleus of the stato-acusticus nerve (VIII d) | + + + | + | + + |
| Ventral nucleus of the stato-acusticus nerve (VIII v) | + + + | + | + + |
| Nucleus of the glossopharyngeal nerve (IX) | – | – | – |
| Nucleus of the hypoglossal nerve (XII) | – | – | + |

Signal density: + + +, very high; + +, high; +, moderate; ±, low; –, background level.

Double labeling of HST and GnRH1 in the frog diencephalon

Double labeling of diencephalic slices with the rabbit HST antiserum and the sheep GnRH1 antiserum, combined with dual-channel CLSM analysis, revealed the presence of GnRH1-positive varicosities in close vicinity with HST-immunoreactive cell bodies in Poa (Figure 4, A and B). Similarly, in Mgd, HST-positive perikarya were apposed by beaded GnRH-immunoreactive processes (Figure 4C). No fluorescence was observed in the negative controls (data not shown). Preincubation of the GnRH1 antiserum with graded concentrations of synthetic GnRH1 (10^{-9} to 10^{-4} M) resulted in a dose-dependent decrease of the immunoreaction with total extinction at a concentration of 10^{-5} M whereas the immunolabeling persisted after preincubation with synthetic GnRH2 (Supplemental Figure 2).

Effect of GnRH1 on biosynthesis of sulfated neurosteroids

Frog hypothalamic slices were incubated for 2 hours with both [^3H] $\Delta^5\text{P}$ as a steroid precursor and [^{35}S]PAPS as a sulfate donor, and the tissue extracts were analyzed by reversed-phase HPLC. The HPLC gradient used made it possible to resolve several double-labeled metabolites (sulfated steroids) including [^3H , ^{35}S] $\Delta^5\text{PS}$, [^3H , ^{35}S]TS, and [^3H , ^{35}S]ES (Figure 5A). Addition of GnRH1 (10^{-6} M) to the incubation medium markedly increased the conver-

sion of [^3H] $\Delta^5\text{P}$ into [^3H , ^{35}S] $\Delta^5\text{PS}$ and reduced the formation of [^3H , ^{35}S]TS, and [^3H , ^{35}S]ES (Figure 5B). Incubation of frog diencephalic slices with graded concentrations of GnRH1 (10^{-8} M to 10^{-5} M) induced a bell-shaped increase of [^3H , ^{35}S] $\Delta^5\text{PS}$ production with a maximum response at a concentration of 10^{-7} M (Figure 5C).

When [^3H]DHEA was used as a precursor, the formation of [^3H , ^{35}S]DHEAS and [^3H , ^{35}S]ES was observed (Figure 6A). Addition of GnRH1 (10^{-6} M) to the incubation medium enhanced the conversion of [^3H]DHEA into [^3H , ^{35}S]DHEAS and had no effect on [^3H , ^{35}S]ES (Figure 6B). Incubation of frog diencephalic slices with graded concentrations of GnRH1 (10^{-8} M to 10^{-5} M) induced a dose-dependent increase of the conversion of [^3H]DHEA into [^3H , ^{35}S]DHEAS with a maximum effect at a concentration of 10^{-5} M (Figure 6C).

Discussion

There is ample evidence that steroid hormones and neurosteroids modulate the activity of GnRH neurons (for reviews, see Refs. 49 and 50). In particular, $\Delta^5\text{PS}$ stimulates GnRH release from hypothalamic neurons through allosteric modulation of N-methyl-D-aspartate receptors (51) whereas DHEAS decreases γ -aminobutyric acid-induced activation of GnRH neurons via γ -aminobutyric acid A receptors (52). In contrast, the possible effect of

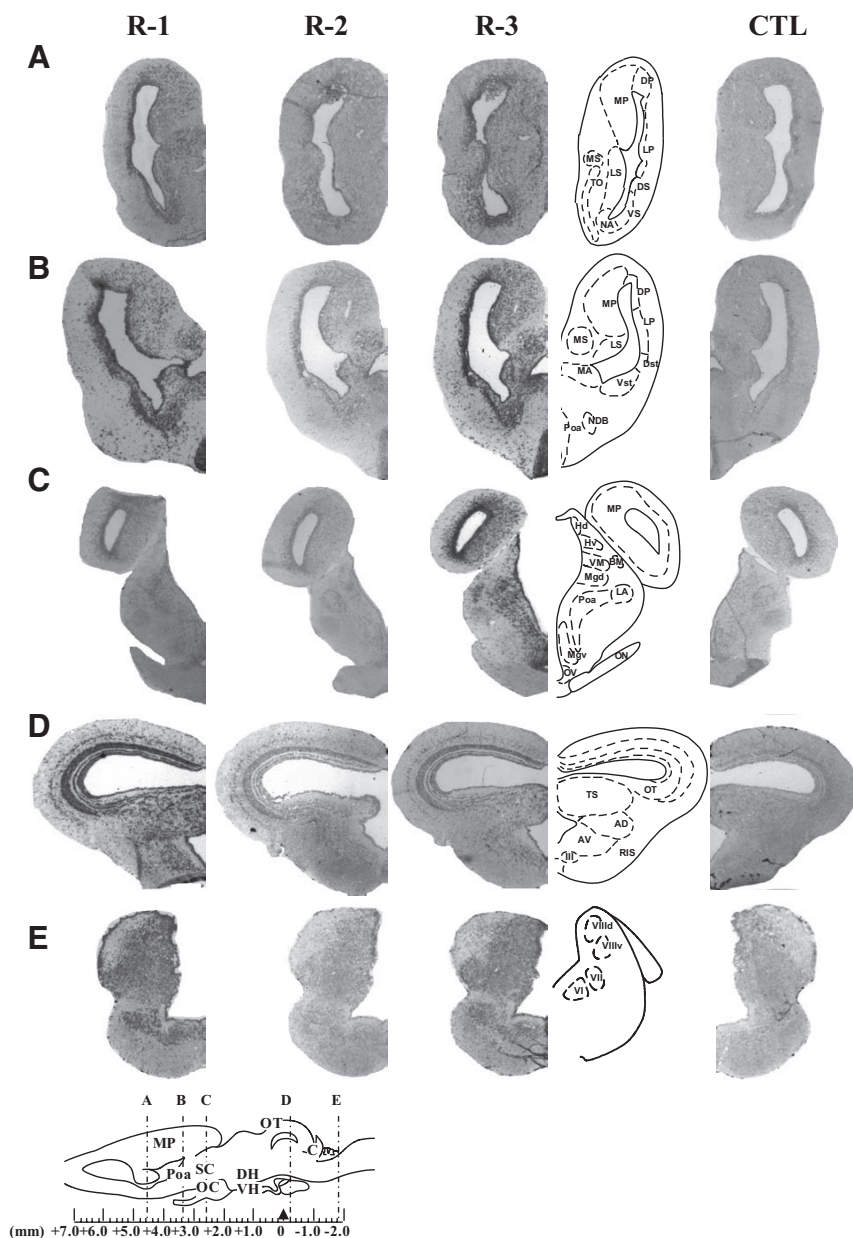


Figure 3. In Situ Hybridization Localization of riGnRHR mRNAs in the Brain A–E, Brain sections were hybridized with ^{35}S -labeled antisense riboprobes for riGnRHR-1 (R-1), riGnRHR-2 (R-2), or riGnRHR-3 (R-3), or riGnRHR-1 sense probe (CTL). The antero-posterior position of the different sections is indicated in the sagittal representation of the frog brain. For abbreviations, see Table 2.

GnRH on the production of neurosteroids has never been investigated. Here, we show that GnRH1 stimulates the biosynthesis of the neurosteroids $\Delta^5\text{PS}$ and DHEAS in the frog diencephalon. Because previous studies describing the cartography of GnRH (30) and HST (21) have been conducted in male frogs, the present experiments were also performed on male animals. In this respect, it has already been reported that the distribution and activity of $17\beta\text{-HSD}$, an enzyme implicated in the biosynthesis of testosterone, are similar in the brain of male and female frogs (53), suggesting that sex steroids do not affect the expression of neurosteroidogenic enzymes in amphibians.

Anatomic relationship between HST-immunoreactive neurons and GnRH-containing nerve fibers

A comparison of the localization patterns of HST- and GnRH1-immunoreactive elements (21, 29) revealed that, in the frog diencephalon, Poa and Mgd, where HST-positive neurons are located, contain a high density of GnRH1-immunoreactive nerve fibers (30). Here, we show by double immunohistochemical labeling that, in these 2 diencephalic nuclei, many HST-expressing perikarya are surrounded by GnRH1-immunoreactive nerve terminals. This observation provided a neuroanatomic clue suggesting that GnRH1 could be involved in the regulation of the biosynthesis of sulfated 3-hydroxy-steroid in the frog diencephalon.

Expression of GnRHRs in the diencephalic nuclei containing HST-immunoreactive neurons

We have cloned the cDNAs encoding three distinct GnRHRs in *P. ridibundus*. riGnRHR-1 and -3 appear to couple preferentially to $G_{q/11}$ whereas riGnRHR-2 has equal potential to activate G_s - and $G_{q/11}$ -mediated signaling pathways. RT-PCR analysis revealed that the 3 riGnRHRs are expressed in all brain regions investigated as well as in the testis, whereas riGnRHR-2 and riGnRHR-3 mRNAs were specifically found in the adrenal gland and in the liver, respectively. In *P. ridibundus* as in *R. castebeyana* (34), riGnRHR-1 is intensely expressed in the distal lobe of the pituitary, suggesting that this receptor plays a major role in the regulation of gonadotrope cells.

The distribution of each receptor mRNA was then determined in the brain by in situ hybridization histochemistry. The results showed that riGnRHR-1 and riGnRHR-3 are actively expressed in the telencephalon and diencephalon, whereas riGnRHR-2 mRNA is mainly localized in the mesencephalon. In fact, the mRNAs for riGnRHR-1 and riGnRHR-3 overlapped in many brain re-

gions. The distribution of each receptor mRNA was then determined in the brain by in situ hybridization histochemistry. The results showed that riGnRHR-1 and riGnRHR-3 are actively expressed in the telencephalon and diencephalon, whereas riGnRHR-2 mRNA is mainly localized in the mesencephalon. In fact, the mRNAs for riGnRHR-1 and riGnRHR-3 overlapped in many brain re-

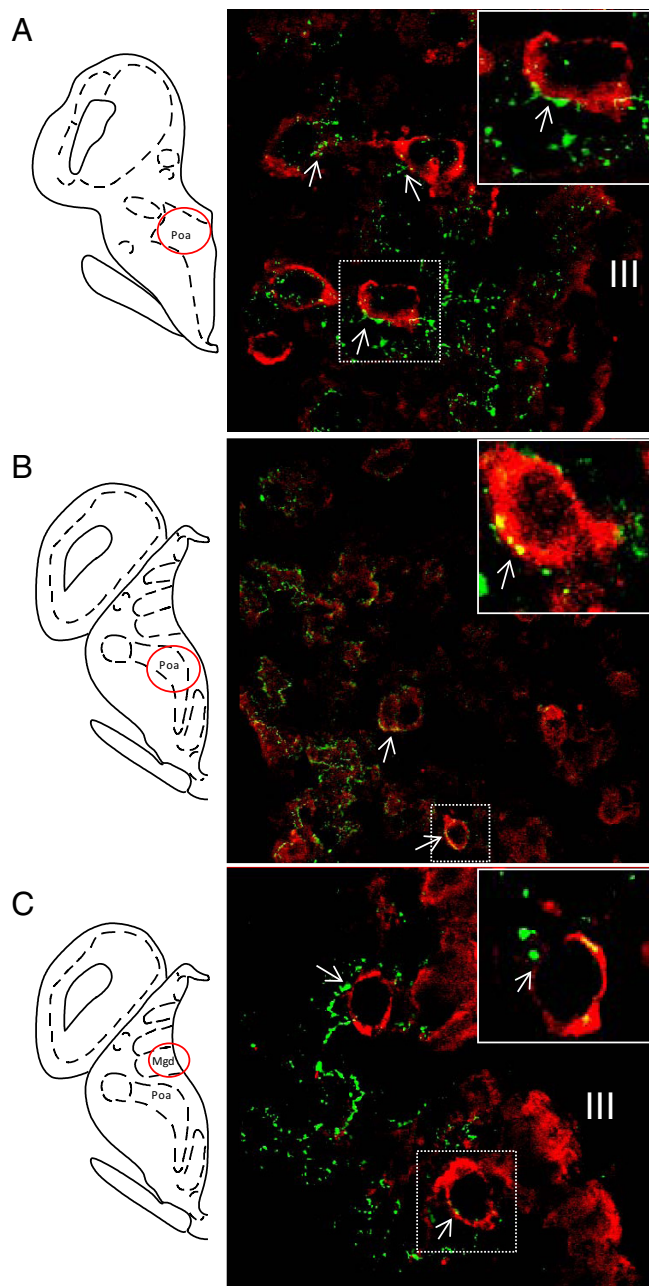


Figure 4. Dual Channel Confocal Laser Scanning Microscope Analysis Of Frontal Sections Of The Frog Brain Illustrating The Distribution of HST- and GnRH1-like immunoreactivity in the Poa (A, $\times 700$; B, $\times 500$) and the Mgd (C, $\times 700$). Each brain section was labeled with a rabbit antiserum against HST revealed with DAR/Texas Red and a sheep antiserum against GnRH1 revealed with DAS/Alexa 488. The Texas Red and Alexa 488 fluorescence signals were analyzed separately using a long-pass filter ($\lambda > 610$ nm) and a band-pass filter ($\lambda = 535$ nm), respectively, and the 2 acquisitions were superimposed on the same image. Arrows point to beaded GnRH1-immunoreactive nerve fibers that are located in the close vicinity of HST-positive neurons. III, third ventricle.

gions. Interestingly, we found that riGnRHR-1 and riGnRHR-3 are actively expressed in Poa and Mgd where HST-immunoreactive neurons are located. These data suggested that GnRH1 might regulate the activity of HST

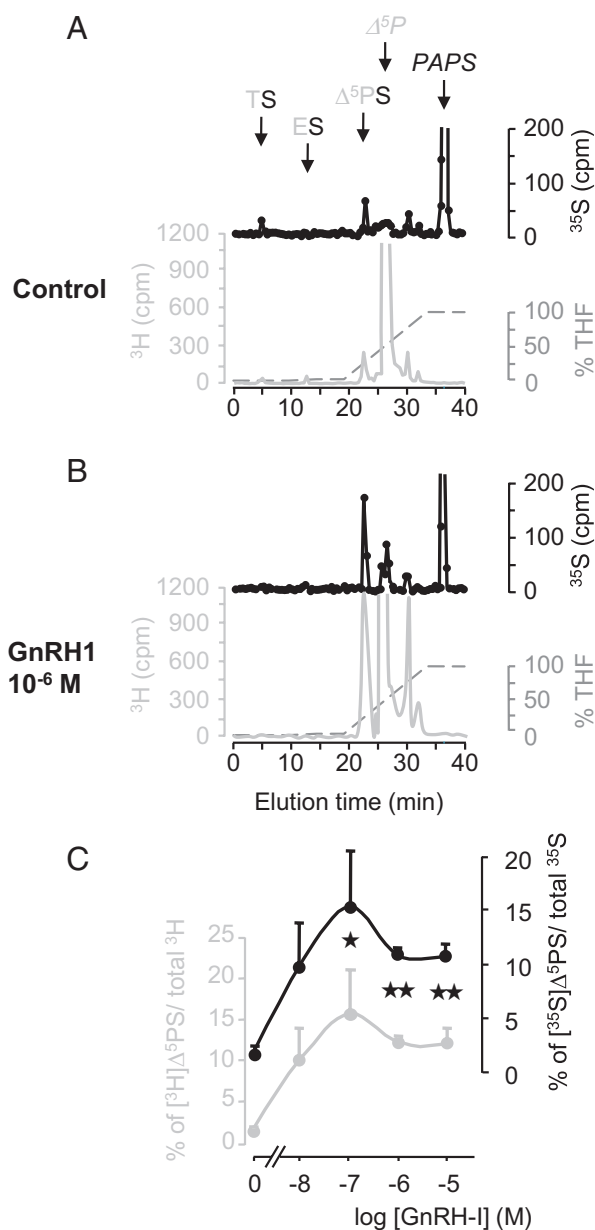


Figure 5. HPLC analysis of Radioactive Metabolites Formed during a 2-hour Incubation Of Frog Hypothalamic Explants with the [^3H]-Labeled Steroid Precursor $\Delta^5\text{P}$ and the [^{35}S]-Labeled Sulfate Donor PAPS. A and B, Frog hypothalamic slices were incubated with 10^{-6} M [^3H] $\Delta^5\text{P}$ together with 4.5×10^{-6} M [^{35}S]PAPS, in the absence (A) or presence (B) of 10^{-6} M GnRH1. The tissues were homogenized and the radioactive metabolites were analyzed using a hexane/THF gradient. The ordinates indicate the radioactivity (^3H and ^{35}S) measured in the HPLC fractions (0.4 mL each). The dashed lines represent the gradient of secondary solvent (% THF). The arrows indicate the elution position of standards: TS, testosterone sulfate. C[b], Effect of graded concentrations of GnRH1 on the conversion of [^3H] $\Delta^5\text{P}$ into [^3H , ^{35}S] $\Delta^5\text{PS}$ by frog hypothalamic explants. The values were obtained from experiments similar to those presented in A and B. Gray circles represent the relative amounts of [^3H] $\Delta^5\text{PS}$ compared with the total amount of [^3H]-labeled compounds resolved by HPLC analysis ($\times 100$). Black circles represent the relative amounts of [^{35}S] $\Delta^5\text{PS}$ compared with the total amount of [^{35}S]-labeled compounds resolved by HPLC analysis ($\times 100$). Each value is the mean (\pm SEM) of three independent experiments. \star , $P < .05$; $\star\star$, $P < .01$.

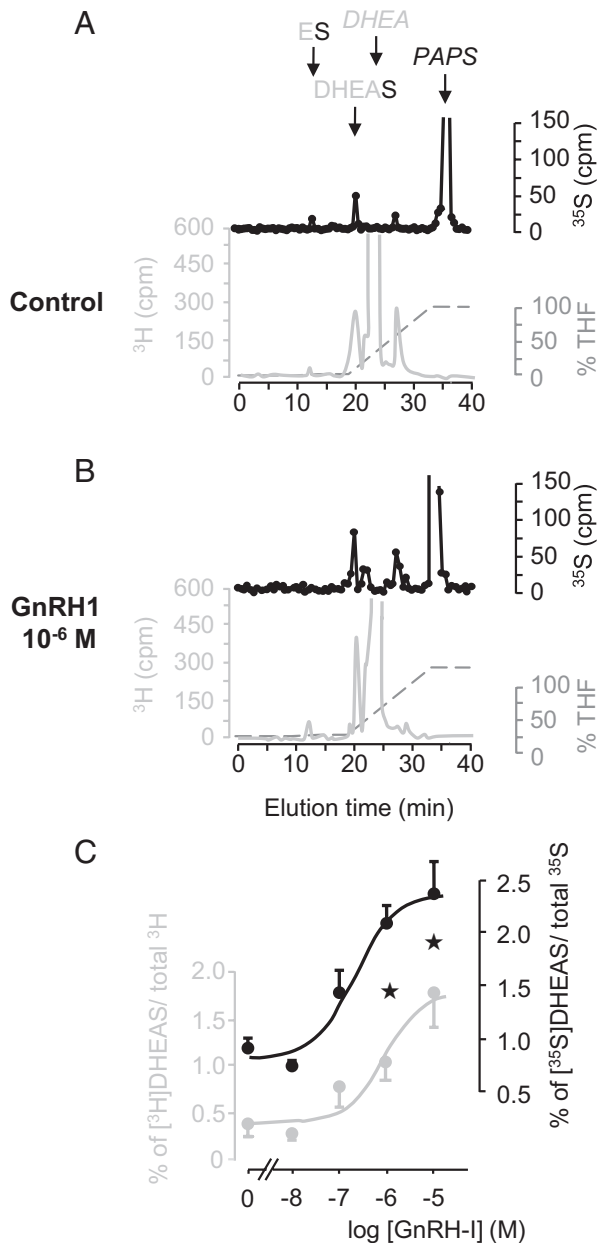


Figure 6. HPLC Analysis of Radioactive Metabolites Formed during a 2-hour Incubation of Frog Hypothalamic Explants with the [³H]-Labeled Steroid Precursor DHEA and the [³⁵S]-Labeled Sulfate Donor PAPS. A and B, Frog hypothalamic slices were incubated with 10⁻⁷ M [³H]DHEA together with 4.5 × 10⁻⁶ M [³⁵S]PAPS, in the absence (A) or presence (B) of 10⁻⁶ M GnRH1. The tissues were homogenized and the radioactive metabolites were analyzed using a hexane/THF gradient. The ordinates indicate the radioactivity (³H and ³⁵S) measured in the HPLC fractions (0.4 mL each). The dashed lines represent the gradient of secondary solvent (% THF). The arrows indicate the elution position of standards ES, estrone sulfate. C, Effect of graded concentrations of GnRH1 on the conversion of [³H]DHEA into [³H,³⁵S]DHEAS by frog hypothalamic explants. The values were obtained from experiments similar to those presented in A and B. Gray circles represent the relative amounts of [³H]DHEAS compared with the total amount of [³H]-labeled compounds resolved by HPLC analysis (×100). Black circles represent the relative amounts of [³⁵S]DHEAS compared with the total amount of [³⁵S]-labeled compounds resolved by HPLC analysis (×100). Each value is the mean (± SEM) of 3 independent experiments. ★, *P* < .05.

neurons through activation of riGnRHR-1 or riGnRHR-3 receptors.

Effect of GnRH1 on sulfated neurosteroid biosynthesis

GnRH1 and GnRH2 are both able to bind and activate the 3 receptors present in hypothalamic nuclei. In agreement with previous results obtained in *R. catesbeiana* and *R. dybowskii* (34, 35), GnRH1 exhibited higher potency on riGnRHR-1 than on riGnRHR-2 and riGnRHR-3, and GnRH2 was slightly more potent than GnRH1 in stimulating c-fos-luc activity in riGnRHR-1-transfected cells. However, because HST-expressing neurons were innervated by GnRH1-containing fibers, we have focused our study on the effect of the GnRH1 isoform on the biosynthesis of sulfated neurosteroids.

Using a pulse-chase approach with [³H]Δ⁵P or [³H]DHEA as a steroid precursor and [³⁵S]PAPS as a sulfate donor (21), we found that GnRH1 stimulates the biosynthesis of [³H]Δ⁵PS and [³H]DHEAS in a concentration-dependent manner. The maximum effect of GnRH1 was observed at a concentration of 10⁻⁷ M for the biosynthesis of Δ⁵PS and 10⁻⁵ M for the biosynthesis of DHEAS. Likewise, it has been previously reported that NPY inhibits Δ⁵PS and DHEAS formation with different potencies (24). These differential effects of GnRH and NPY on Δ⁵PS and DHEAS synthesis may be ascribed to the existence of two HST isoforms in the frog brain. One isoform, more specific for Δ⁵P, would be activated by moderate concentrations of GnRH1 whereas the other isoform, more specific for DHEA, would require higher concentrations of GnRH1 to be stimulated. To the best of our knowledge, this is the first report demonstrating that GnRH stimulates the biosynthesis of steroids in the CNS. The observation that GnRH-immunoreactive fibers were apposed onto HST-expressing cells is in favor of a direct action of GnRH1 on HST neurons although an indirect effect via intermediate neurons cannot be ruled out. As a matter of fact, a recent report indicates that GnRH1 directly activates steroidogenesis in human neuroblastoma and human neuroblast cell lines (54), suggesting that GnRH1 may also exert a stimulatory effect on neurosteroid biosynthesis in the brain of mammals.

The intense expression of riGnRHR-1 and riGnRHR-3 in Poa and Mgd strongly suggests that GnRH1 stimulates the biosynthesis of sulfated neurosteroids through activation of one of these 2 receptors. Our data also revealed the presence of GnRHR-1 and GnRHR-2 mRNAs in the testis and adrenal gland, two major sites of DHEAS production at the periphery. Whether GnRH can also regulate the activity of HST and thus the biosynthesis of sulfated neu-

rosteroids in these steroidogenic glands remains to be determined.

Functional significance

The wide distribution of the 3 GnRHRs in the frog brain is consistent with the multiple roles of GnRH as a neuromodulator and neurotransmitter. Thus, the occurrence of the 3 receptors in the striatum suggests that GnRH could modulate various sensory pathways. In amphibians, the striatum actually receives visual, olfactory, and auditory information and represents the major telencephalic output to the mesencephalon (55). The presence of GnRHRs in the tegmentum, optic tectum, oculomotor, and trochlear nuclei, as well as in the nucleus of the medial longitudinal fasciculus, indicates that GnRH may influence amphibian visually guided behaviors (56) as previously demonstrated in fish (57) and birds (58). Moreover, the expression of all riGnRHRs in the nucleus of the statoacoustic nerve and in the torus semicircularis provides additional evidence for an auditory-endocrine circuit that involves GnRH1 and GnRH2 systems (59, 60). Finally, the presence of riGnRHRs in the pallium and the medial amygdala, considered as olfactory centers in frog, supports the hypothesis of a role of GnRH1 and/or GnRH2 in olfaction in amphibians (61, 62). Concerning reproductive behavior, the occurrence of riGnRHR-1 and riGnRHR-3 in the ventral telencephalon, an area known to be involved in spawning behavior (63), may account for the stimulatory effect of GnRH2 on female spawning behavior (64).

Unlike the lipophilic nonconjugated steroid hormones that can enter easily into the brain, steroid ester sulfates, due to their hydrophilic nature, can hardly cross the blood-brain barrier. In fact, the concentration of Δ^5 PS in frog brain tissue is 3 to 15 times higher than in plasma (39), indicating that sulfated steroids present in the CNS are synthesized locally. It has also been reported that, in frog, the concentration of Δ^5 PS in the brain undergoes seasonal variations that are totally dissociated from plasma Δ^5 PS levels (39), suggesting the existence of a tight regulation of the activity of the enzymes responsible for the production of steroid sulfates in the CNS. Consistent with this hypothesis, we have previously shown that, in the frog diencephalon, NPY inhibits the formation of sulfated steroids through activation of Y1 receptors (24). The present data now indicate that GnRH1 stimulates the biosynthesis of Δ^5 PS and DHEAS likely through activation of riGnRHR-1 and/or GnRHR-3. Because the concentrations of GnRH1 and Δ^5 PS are elevated in the brain of amphibians at the beginning of the breeding season (38, 65), it is tempting to speculate that the stimulatory effect of GnRH1 on amplexus behavior (66) is mediated by Δ^5 PS. Recipro-

cally, Δ^5 PS and DHEAS modulate the activity of GnRH neurons (51, 52), suggesting the existence of a short feedback regulatory loop between the two neuronal systems.

In conclusion, the frog brain contains 3 different types of GnRHRs. The widespread distribution of these riGnRHRs supports the view that GnRH acts as a neurotransmitter and neuromodulator in addition to its well-known neuroendocrine functions. In agreement with this hypothesis, our data show that GnRH stimulates the biosynthesis of Δ^5 PS and DHEAS in the frog hypothalamus, suggesting that some of the neurobiologic effects of GnRH can be accounted for by stimulation of HST bioactivity.

Acknowledgments

Address all correspondence and requests for reprints to: Dr Jae Young Seong, Laboratory of G-Protein-Coupled Receptors, Graduate School of Medicine, Korea University, 126-1 Anam 5-ga, Seongbuk, Seoul 136-705, Republic of Korea; E-mail: jyseong@korea.ac.kr; or Dr Hubert Vaudry, Research Institute for Biomedicine (IRIB), Laboratory of Neuronal and Neuroendocrine Differentiation and Communication, Institut National de la Santé et de la Recherche Médicale U982, University of Rouen, 76821 Mont-Saint-Aignan, France; E-mail: hubert.vaudry@univ-rouen.fr.

This work was supported by a grant from the Brain Research Program of the National Research Foundation of Korea (NRF) funded by the Ministry of Education, Science, and Technology (2011-0019205) to J.Y.S., a grant from Institut National de la Santé et de la Recherche Médicale (INSERM) (U413) to H.V., a France-Korea (STAR) exchange program (to J.Y.S. and H.V.), a France-Québec (FRSQ-INSERM) exchange program (to G.P. and H.V.), the Ministère de l'Enseignement Supérieur et de la Recherche, and the Région Haute-Normandie.

Disclosure Summary: The authors have nothing to disclose.

References

1. Rupperecht R, Holsboer F. Neuroactive steroids: mechanisms of action and neuropsychopharmacological perspectives. *Trends Neurosci.* 1999;22:410–416.
2. Tsutsui K, Ukena K, Usui M, Sakamoto H, Takase M. Novel brain function: biosynthesis and actions of neurosteroids in neurons. *Neurosci Res.* 2000;36:261–273.
3. Baulieu EE, Robel P, Schumacher M. Neurosteroids: beginning of the story. *Int Rev Neurobiol.* 2001;46:1–32.
4. Chen L, Miyamoto Y, Furuya K, Mori N, Sokabe M. PREGS induces LTP in the hippocampal dentate gyrus of adult rats via the tyrosine phosphorylation of NR2B coupled to ERK/CREB signaling [published correction appears in *J Neurophysiol.* 2007;98:3120]. *J Neurophysiol.* 2007;98:1538–1548.
5. Vallée M, Mayo W, Le Moal M. Role of pregnenolone, dehydroepiandrosterone and their sulfate esters on learning and memory in cognitive aging. *Brain Res Rev.* 2001;37:301–312.
6. Akwa Y, Ladurelle N, Covey DF, Baulieu EE. The synthetic enantiomer of pregnenolone sulfate is very active on memory in rats and

- mice, even more so than its physiological neurosteroid counterpart: distinct mechanisms? *Proc Natl Acad Sci USA*. 2001;98:14033–14037.
7. Mao X, Barger SW. Neuroprotection by dehydroepiandrosterone sulfate: role of an NF κ B-like factor. *Neuroreport*. 1998;9:759–763.
 8. Kurata K, Takebayashi M, Morinobu S, Yamawaki S. β -estradiol, dehydroepiandrosterone, and dehydroepiandrosterone sulfate protect against N-methyl-D-aspartate-induced neurotoxicity in rat hippocampal neurons by different mechanisms. *J Pharmacol Exp Ther*. 2004;311:237–245.
 9. Milman A, Zohar O, Maayan R, Weizman R, Pick CG. DHEAS repeated treatment improves cognitive and behavioral deficits after mild traumatic brain injury. *Eur Neuropsychopharmacol*. 2008;18:181–187.
 10. Yoon SY, Roh DH, Seo HS, et al. Intrathecal injection of the neurosteroid, DHEAS, produces mechanical allodynia in mice: involvement of spinal sigma-1 and GABA receptors. *Br J Pharmacol*. 2009;157:666–673.
 11. Corpéchet C, Robel P, Axelson M, Sjövall J, Baulieu EE. Characterization and measurement of dehydroepiandrosterone sulfate in rat brain. *Proc Natl Acad Sci USA*. 1981;78:4704–4707.
 12. Corpéchet C, Synguelakis M, Talha S, et al. Pregnenolone and its sulfate ester in the rat brain. *Brain Res*. 1983;270:119–125.
 13. Mathur C, Prasad VV, Raju VS, Welch M, Lieberman S. Steroids and their conjugates in the mammalian brain. *Proc Natl Acad Sci USA*. 1993;90:85–88.
 14. Knapstein P, David A, Wu CH, Archer DF, Flickinger GL, Tochstone JC. Metabolism of free and sulfoconjugated DHEA in brain tissue in vivo and in vitro. *Steroids*. 1968;11:885–896.
 15. Rajkowski KM, Robel P, Baulieu EE. Hydroxysteroid sulfotransferase activity in the rat brain and liver as a function of age and sex. *Steroids*. 1997;62:427–436.
 16. Griffiths WJ, Liu S, Yang Y, Purdy RH, Sjövall J. Nano-electrospray tandem mass spectrometry for the analysis of neurosteroid sulphates. *Rapid Commun Mass Spectrom*. 1999;13:1595–1610.
 17. Higashi T, Daifu Y, Shimada K. Studies on neurosteroids XIV. Levels of dehydroepiandrosterone sulfate in rat brain and serum determined with newly developed enzyme-linked immunosorbent assay. *Steroids*. 2001;66:865–874.
 18. Higashi T, Sugitani H, Yagi T, Shimada K. Studies on neurosteroids XVI. Levels of pregnenolone sulfate in rat brains determined by enzyme-linked immunosorbent assay not requiring solvolysis. *Biol Pharm Bull*. 2003;26:709–711.
 19. Liu S, Sjövall J, Griffiths WJ. Neurosteroids in rat brain: extraction, isolation, and analysis by nanoscale liquid chromatography-electrospray mass spectrometry. *Anal Chem*. 2003;75:5835–5846.
 20. Sharp S, Barker EV, Coughtrie MW, Lowenstein PR, Hume R. Immunochemical characterisation of a dehydroepiandrosterone sulfotransferase in rats and humans. *Eur J Biochem*. 1993;211:539–548.
 21. Beaujean D, Mensah-Nyagan AG, Do-Rego JL, Luu-The V, Pelletier G, Vaudry H. Immunocytochemical localization and biological activity of hydroxysteroid sulfotransferase in the frog brain. *J Neurochem*. 1999;72:848–857.
 22. Cevalco A, Pittaluga A, Do Rego JL, et al. Immunohistochemical localization of hydroxysteroid sulfotransferase and sulfatase in the brain of *Rana esculenta* tadpoles. *Ann NY Acad Sci*. 2009;1163:365–368.
 23. Do-Rego JL, Seong JY, Burel D, et al. Neurosteroid biosynthesis: enzymatic pathways and neuroendocrine regulation by neurotransmitters and neuropeptides. *Front Neuroendocrinol*. 2009;30:259–301.
 24. Beaujean D, Do-Rego JL, Galas L, et al. Neuropeptide Y inhibits the biosynthesis of sulfated neurosteroids in the hypothalamus through activation of Y(1) receptors. *Endocrinology*. 2002;143:1950–1963.
 25. Matsuo H, Baba Y, Nair RM, Arimura A, Schally AV. Structure of the porcine LH- and FSH-releasing hormone. I. The proposed amino acid sequence. *Biochem Biophys Res Commun*. 1971;43:1334–1339.
 26. Burgus R, Butcher M, Amoss M, et al. Primary structure of the ovine hypothalamic luteinizing hormone-releasing factor (LRF) (LH-hypothalamus-LRF-gas chromatography-mass spectrometry-decapeptide-Edman degradation). *Proc Natl Acad Sci USA*. 1972;69:278–282.
 27. Kim DK, Cho EB, Moon MJ, et al. Revisiting the evolution of gonadotropin-releasing hormones and their receptors in vertebrates: secrets hidden in genomes. *Gen Comp Endocrinol*. 2011;170:68–78.
 28. Conlon JM, Kolodziejek J, Nowotny N. Antimicrobial peptides from the skins of North American frogs. *Biochim Biophys Acta*. 2009;1788:1556–1563.
 29. Conlon JM, Collin F, Chiang YC, Sower SA, Vaudry H. Two molecular forms of gonadotropin-releasing hormone from the brain of the frog, *Rana ridibunda*: purification, characterization, and distribution. *Endocrinology*. 1993;132:2117–2123.
 30. Collin F, Chartrel N, Fasolo A, Conlon JM, Vandesande F, Vaudry H. Distribution of two molecular forms of gonadotropin-releasing hormone (GnRH) in the central nervous system of the frog *Rana ridibunda*. *Brain Res*. 1995;703:111–128.
 31. Lethimonier C, Madigou T, Muñoz-Cueto JA, Lareyre JJ, Kah O. Evolutionary aspects of GnRHs, GnRH neuronal systems and GnRH receptors in teleost fish. *Gen Comp Endocrinol*. 2004;135:1–16.
 32. Moncaut N, Somoza G, Power DM, Canário AV. Five gonadotropin-releasing hormone receptors in a teleost fish: isolation, tissue distribution and phylogenetic relationships. *J Mol Endocrinol*. 2005;34:767–779.
 33. Millar R, Lowe S, Conklyn D, et al. A novel mammalian receptor for the evolutionarily conserved type II GnRH. *Proc Natl Acad Sci USA*. 2001;98:9636–9641.
 34. Wang L, Bogerd J, Choi HS, et al. Three distinct types of GnRH receptor characterized in the bullfrog. *Proc Natl Acad Sci USA*. 2001;98:361–366.
 35. Seong JY, Wang L, Oh DY, et al. Ala/Thr(201) in extracellular loop 2 and Leu/Phe(290) in transmembrane domain 6 of type 1 frog gonadotropin-releasing hormone receptor confer differential ligand sensitivity and signal transduction. *Endocrinology*. 2003;144:454–466.
 36. Kavaliers M, Kinsella DM. Male preference for the odors of estrous female mice is reduced by the neurosteroid pregnenolone sulfate. *Brain Res*. 1995;682:222–226.
 37. Sagrillo CA, Grattan DR, McCarthy MM, Selmanoff M. Hormonal and neurotransmitter regulation of GnRH gene expression and related reproductive behaviors. *Behav Genet*. 1996;26:241–277.
 38. Tsutsui K, Bentley GE, Kriegsfeld LJ, Osugi T, Seong JY, Vaudry H. Discovery and evolutionary history of gonadotrophin-inhibitory hormone and kisspeptin: new key neuropeptides controlling reproduction. *J Neuroendocrinol*. 2010;22:716–727.
 39. Takase M, Ukena K, Yamazaki T, Kominami S, Tsutsui K. Pregnenolone, pregnenolone sulfate, and cytochrome P450 side-chain cleavage enzyme in the amphibian brain and their seasonal changes. *Endocrinology*. 1999;140:1936–1944.
 40. Koyama T, Haraguchi S, Vaudry H, Tsutsui K. Diurnal changes in the synthesis of the neurosteroid 7 α -hydroxypregnenolone stimulating locomotor activity in newts. *Ann NY Acad Sci*. 2009;1163:444–447.
 41. Ogura K, Kajita J, Narihata H, et al. Cloning and sequence analysis of a rat liver cDNA encoding hydroxysteroid sulfotransferase. *Biochem Biophys Res Commun*. 1989;165:168–174.
 42. Molter-Gérard C, Caraty A, Guérin S, Fontaine J, Taragnat C. Dynamic changes in the gonadotrope cell subpopulations during an estradiol-induced surge in the ewe. *Biol Reprod*. 2000;63:1084–1091.

43. Kakar SS. Molecular structure of the human gonadotropin-releasing hormone receptor gene. *Eur J Endocrinol.* 1997;137:183–192.
44. Troskie BE, Hapgood JP, Millar RP, Illing N. Complementary deoxyribonucleic acid cloning, gene expression, and ligand selectivity of a novel gonadotropin-releasing hormone receptor expressed in the pituitary and midbrain of *Xenopus laevis*. *Endocrinology.* 2000;141:1764–1771.
45. Wang L, Oh DY, Bogerd J, et al. Inhibitory activity of alternative splice variants of the bullfrog GnRH receptor-3 on wild-type receptor signaling. *Endocrinology.* 2001;142:4015–4025.
46. Wang L, Yoo MS, Kang HM, et al. Cloning and characterization of cDNAs encoding the GnRH1 and GnRH2 precursors from bullfrog (*Rana catesbeiana*). *J Exp Zool.* 2001;289:190–201.
47. Jolivel V, Basille M, Aubert N, et al. Distribution and functional characterization of pituitary adenylate cyclase-activating polypeptide receptors in the brain of non-human primates. *Neuroscience.* 2009;160:434–451.
48. Neary TJ, Northcutt RG. Nuclear organization of the bullfrog diencephalon. *J Comp Neurol.* 1983;213:262–278.
49. Krsmanovic LZ, Hu L, Leung PK, Feng H, Catt KJ. The hypothalamic GnRH pulse generator: multiple regulatory mechanisms. *Trends Endocrinol Metab.* 2009;20:402–408.
50. Clarke IJ. Control of GnRH secretion: one step back. *Front Neuroendocrinol.* 2011;32:367–375.
51. El-Etr M, Akwa Y, Baulieu EE, Schumacher M. The neuroactive steroid pregnenolone sulfate stimulates the release of gonadotropin-releasing hormone from GT1-7 hypothalamic neurons, through N-methyl-D-aspartate receptors. *Endocrinology.* 2006;147:2737–2743.
52. Sullivan SD, Moenter SM. Neurosteroids alter γ -aminobutyric acid postsynaptic currents in gonadotropin-releasing hormone neurons: a possible mechanism for direct steroidal control. *Endocrinology.* 2003;144:4366–4375.
53. Mensah-Nyagan AG, Do-Rego JL, Feuilleux M, et al. In vivo and in vitro evidence for the biosynthesis of testosterone in the telencephalon of the female frog. *J Neurochem.* 1996;67:413–422.
54. Rosati F, Sturli N, Cungi MC, et al. Gonadotropin-releasing hormone modulates cholesterol synthesis and steroidogenesis in SH-SY5Y cells. *J Steroid Biochem Mol Biol.* 2011;124:77–83.
55. Birkhofer M, Bleckmann H, Görner P. Sensory activity in the telencephalon of the clawed toad, *Xenopus laevis*. *Eur J Morphol.* 1994;32:262–266.
56. Wu GY, Wang SR. Postsynaptic potentials and axonal projections of tegmental neurons responding to electrical stimulation of the toad striatum. *Neurosci Lett.* 2007;429:111–114.
57. Ramakrishnan S, Wayne NL. Social cues from conspecifics alter electrical activity of gonadotropin-releasing hormone neurons in the terminal nerve via visual signals. *Am J Physiol Regul Integr Comp Physiol.* 2009;297:R135–R141.
58. Meddle SL, Wingfield JC, Millar RP, Deviche PJ. Hypothalamic GnRH-I and its precursor during photorefractoriness onset in free-living male Dark-eyed Juncos (*Junco hyemalis*) of different year classes. *Gen Comp Endocrinol.* 2006;145:148–156.
59. Burmeister SS, Wilczynski W. Social signals regulate gonadotropin-releasing hormone neurons in the green treefrog. *Brain Behav Evol.* 2005;65:26–32.
60. Maruska KP, Tricas TC. Gonadotropin-releasing hormone (GnRH) modulates auditory processing in the fish brain. *Horm Behav.* 2011;59:451–564.
61. Eisthen HL, Delay RJ, Wirsig-Wiechmann CR, Dionne VE. Neuromodulatory effects of gonadotropin releasing hormone on olfactory receptor neurons. *J Neurosci.* 2000;20:3947–3955.
62. Zhang W, Delay RJ. Gonadotropin-releasing hormone modulates voltage-activated sodium current and odor responses in *Necturus maculosus* olfactory sensory neurons. *J Neurosci Res.* 2007;85:1656–1667.
63. Kyle AL, Stacey NE, Peter RE. Ventral telencephalic lesions: effects on bisexual behavior, activity, and olfaction in the male goldfish. *Behav Neural Biol.* 1982;36:229–241.
64. Volkoff H, Peter RE. Actions of two forms of gonadotropin releasing hormone and a GnRH antagonist on spawning behavior of the goldfish *Carassius auratus*. *Gen Comp Endocrinol.* 1999;116:347–355.
65. Zoeller RT, Moore FL. Seasonal changes in luteinizing hormone-releasing hormone concentrations in microdissected brain regions of male rough-skinned newts (*Taricha granulosa*). *Gen Comp Endocrinol.* 1985;58:222–230.
66. Propper CR, Dixon TB. Differential effects of arginine vasotocin and gonadotropin-releasing hormone on sexual behaviors in an anuran amphibian. *Horm Behav.* 1997;32:99–104.